ACTA ONCOLOGICA
2023, VOL. 62, NO. 8, 915–922
https://doi.org/10.1080/0284186X.2023.2238556

Taylor & Francis
Taylor & Francis Group

ORIGINAL ARTICLE

Experimental validation of a novel method of dose accumulation for the rectum

H. M. Patrick[a], E. Poon[b] and J. Kildea[a,c]

[a]Medical Physics Unit, McGill University, Montreal, Québec, Canada; [b]Department of Medical Physics, McGill University Health Centre, Montreal, Québec, Canada; [c]Cancer Research Program, Research Institute of the McGill University Health Centre, Montreal, Québec, Canada

ABSTRACT

Background: Dose-surface maps (DSMs) are an increasingly popular tool to evaluate spatial dose-outcome relationships for the rectum. Recently, DSM addition has been proposed as an alternative method of dose accumulation from deformable registration-based techniques. In this study, we performed the first experimental investigation of the accuracy at which DSM accumulation can capture the total dose delivered to a rectum's surface in the presence of inter-fraction motion.

Material and methods: A custom PVC rectum phantom capable of representing typical rectum inter-fraction motion and filling variations was constructed for this project. The phantom allowed for the placement of EBT3 film sheets on the representative rectum surface to measure rectum surface dose. A multi-fraction prostate VMAT treatment was designed and delivered to the phantom in a water tank for a variety of inter-fraction motion scenarios. DSMs for each fraction were calculated in two ways using CBCT images acquired during delivery and summed to produce accumulated DSMs. Accumulated DSMs were then compared to film measurements using gamma analysis (3%/2 mm criteria). Similarity of isodose clusters between films and DSMs was also investigated.

Results: Baseline agreement between film measurements and accumulated DSMs for a stationary rectum was 95.6%. Agreement between film and accumulated DSMs in the presence of different types of inter.-fraction motion was $\geq$92%, and isodose cluster mean distance to agreement was within 1.5 mm for most scenarios. Overall, DSM accumulation performed the best when using DSMs that accounted for changes in rectum path orientation.

Conclusion: Dose accumulation performed with DSMs was found to accurately replicate total delivered dose to a rectum phantom in the presence of inter-fraction motion.

ARTICLE HISTORY
Received 23 March 2023
Accepted 8 July 2023

KEYWORDS
Dose-surface maps; dose accumulation; prostate radiotherapy; film dosimetry

Background

Dose-surface maps (DSMs) are sources of spatial dose distribution information in radiation oncology that are becoming increasingly popular for dose-outcome studies of hollow organs like the rectum [1,2], with growing interest in using them to evaluate delivered dose to the rectum [3,4]. However, accurate quantification of delivered dose to the rectum can be challenging. While Murray et al. were the first to use DSMs to perform dose accumulation for the rectum several years ago [5], no attempt to experimentally test the validity of this approach has been made. Considering that interest in using DSMs for dose accumulation appears to be growing [3,6,7], an evaluation of its validity is warranted.

During a course of prostate radiotherapy the shapes and positions of organs within the irradiated volume can change substantially due to inter-fraction motion, with reported prostate shifts on the order of 2.7–15 mm [8–10]. Failure to account for this motion can introduce discrepancies between planned and delivered dose to the target and organs at risk (OARs) and has been shown to contribute to increased risk of relapse and radiation toxicities in conformal treatments [11–14]. While daily image-guided radiotherapy (IGRT) is able restrict dose deviations to the prostate target to within 4%, delivered dose to the rectum and bladder can still differ substantially from what was planned [15], necessitating a means to determine the dose that was delivered.

Dose accumulation is a process that uses a patient's treatment plan and daily IGRT images to calculate and sum their daily delivered doses into a total, accumulated dose. As anatomical variations can exist between treatment fractions, a key element of dose accumulation is a means to combine daily doses in the same reference anatomy. Traditionally, this is achieved using deformable image registration (DIR) algorithms to deform daily images to the planning anatomy along with their daily dose distributions. However, many DIR algorithms are unable to properly handle the complex deformations and filling changes of the rectum during prostate radiotherapy [16–18]. Although some performance improvements have been reported for newer hybrid or biomechanical deformation algorithms [19–21], DIR's historically weak performance for the rectum has led to the investigation of alternative dose accumulation strategies for this organ.

As mentioned earlier, a growing number of groups are reporting on rectum dose accumulation for dose-outcome

CONTACT H. M. Patrick haley.patrick@mail.mcgill.ca Medical Physics Unit, McGill University, Montreal, Québec, Canada
Supplemental data for this article can be accessed online at https://doi.org/10.1080/0284186X.2023.2238556.
This article has been corrected with minor changes. These changes do not impact the academic content of the article.

studies using DSMs [4,7,22]. A DSM is a 2D representation of the dose to the surface of an organ. DSMs are typically calculated in a way that maps the dose to an organ's surface to a standard grid, making dose accumulation as hypothetically simple as superimposing and adding daily DSMs together. However, this daily DSM addition process relies on the untested assumption that it can accurately account for inter-fraction translations and volume variations to produce accurate accumulated doses. Considering that empirical studies of DIR performance for dose deformation have revealed important real-world inconsistencies that were not observable in prior *in silico* studies [23], similar real-world validation of DSM-based dose accumulation is essential if it is to become a viable dose accumulation technique.

Motivated by this need, in this study, we attempted to validate DSM-based dose accumulation for the rectum. Inter-fraction rectal motion and distension over the course of a multi-fraction treatment were simulated using a rudimentary pelvic phantom and the accuracy of accumulated DSM dose accumulation was assessed using EBT3 film dosimetry.

Materials and methods

Phantom design

A $28 \times 28 \times 29$ cm acrylic water tank was used as a simple pelvic phantom, with interchangeable 15 cm lengths of Xirtec® PVC pipe of various diameters used to represent the rectum within it (Figure 1a). Radiopaque BBs and etched crosshairs on the tank were used to facilitate reproducible setup of the tank's center with in-room patient-positioning lasers. Water level markers were also added to ensure reproducible tank filling. Pipe diameters of $^3/_4''$, $1''$, and $1\ ^1/_4''$ were used to represent the range of rectum cross sectional areas reported in the literature [24]. In order to reproduce the rectum's anatomical position in a supine patient, a custom stand insert was constructed to interchangeably hold each rectum pipe 9 cm above the tank's base. This positioned the rectum pipe's anterior wall 2.5 cm posterior to the positioning of the isocenter within the tank, replicating the average distance between the rectum and the isocenter location in prostate cancer treatment plans. Both the rectum pipes and the stand were marked with guide lines to allow for easy alignment with the lasers (detailed protocol provided in Supplemental Materials). Pipe positions could also be varied by using different height stands or shimming the stand's base plate.

Treatment planning

A CT simulation image of the phantom containing the smallest diameter (reference) pipe was taken using a Big Bore CT scanner (Philips, Amsterdam, The Netherlands) with a 3.0 mm slice thickness and imported into Eclipse (v.15, Varian Medical Systems Palo Alto, CA) for treatment planning. The tank 'body' and rectum pipe were contoured and a 5.5 cm diameter spherical PTV defined at the isocenter location. A 6 MV two-arc VMAT plan was designed based on our institutional 60 Gy in 20 fractions treatment for moderate-risk prostate cancer [25]. In brief, the prescription was reduced to

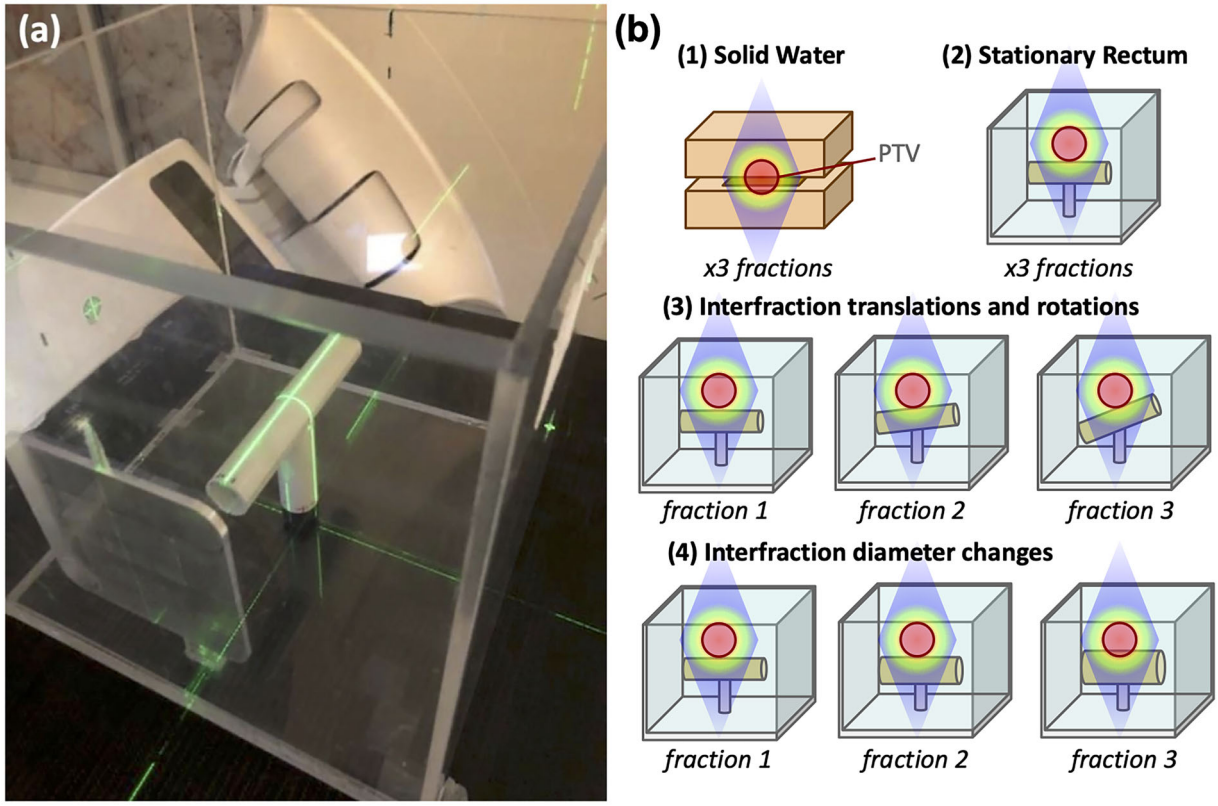

Figure 1. (a) Set-up of the water tank with the smallest diameter rectum pipe in place. (b) Visualizations of the four measurement set-ups tested in this study, with the faux-prostate PTV (red circle) and dose distributions included for dosimetric context.

3 Gy in 3 fractions and the planning constraints for the rectum and PTV were scaled down accordingly. The 3 Gy prescription dose was chosen as it provided the least noisy dose distributions in our EBT3 films of the prescriptions tested.

Experimental setups

All measurements were performed on a Varian TrueBeam linac. In total, four different measurements were performed to evaluate the agreement between film and calculated DSMs. Each represented a different scenario of interest as follows (Figure 1b):

1. Dose plane in solid water: used to evaluate the baseline agreement between the treatment plan and its delivery using a standard film IMRT QA protocol [26]. Two 30 x 30 x 6 cm slabs of solid water were positioned on the treatment couch with a 127×203 mm sheet of film sandwiched between them, centered at the isocenter, and irradiated with the three-fraction treatment plan.
2. Dose to a stationary rectum: used to evaluate the baseline agreement between a DSM and film measurement. The center of the water-filled water tank was positioned at the isocenter, a 127×85mm sheet of film was secured tightly around the circumference of the smallest diameter rectum pipe and centered on the stand using the room lasers. The plan was delivered in its entirety to the phantom, after which the film was removed, gently toweled dry, and stored to develop.
3. Dose to a rectum with inter-fraction motion: used to evaluate how well accumulated DSMs represent delivered dose in scenarios involving inter-fraction translation/rotation. The set-up was identical to measurement 2, except that the film and pipe were further secured to the stand with tape to prevent motion during fractions. Between the delivery of each fraction the pipe stand was shimmed, tilting the pipe 3°, then 7° from horizontal.
4. Dose to a rectum with inter-fraction volume changes: used to evaluate how well accumulated DSMs calculate delivered dose for scenarios that involve rectum diameter changes. As the different diameters made it impossible for a single film sheet to measure the accumulated surface dose across all three fractions, we opted to measure accumulated dose to four inferior-superior lines located at the cardinal angles along the rectum's surface. Four 127×20mm strips of film were attached to the posterior, anterior, left, and right sides of each rectum pipe and centered in the tank using the room lasers. After each fraction the films were removed and transferred to a different diameter pipe for delivery of the next fraction.

Before each film measurement, a CBCT image of the experimental set-up was acquired with a dummy film in the place of the measurement film to facilitate the delivered dose and DSM calculation processes. In order to assess and account for any film darkening due to water, each water tank measurement had a corresponding non-irradiated reference film submerged for the same duration as the measurement film. This reference film was scanned alongside the measurement films and a piece of non-submerged film, and compared to the non-submerged film. Significant water-induced darkening could then be accounted for by subtracting the difference in optical density from measurement films [27].

Film dosimetry

All measurements were carried out using Gafcromic EBT3 film (Ashland Global, Lot 03082202). Film calibration was performed by exposing film strips positioned at 6 cm depth in solid water using a 6 MV 10×10cm, 100 cm SSD field. Six calibration doses covering a range from 0 to 500 cGy were acquired and cross-calibrated with measurements performed with an Exradin® A19 ion chamber. All films were left to develop for 42 h to allow for full evaporation of water from submerged films before scanning in 48-bit RGB format with an Epson 11000XL scanner and glass compression plate at 0.35 mm resolution. Images were converted to dose distributions using FilmQA Pro (v.5, Ashland Global) [28]. Measurement films were scanned alongside three reference films: the aforementioned submerged film (0 cGy) and two non-submerged films irradiated to 0 and 400 cGy in the same solid water setup as the calibration films. The two 0 cGy films were used to account for water-induced darkening, while the two non-submerged films were used to perform linear dose rescaling to correct for inter-scan variability. No additional post-processing was performed.

Dose-surface map calculation and accumulation

For each measurement scenario, delivered dose was calculated by first registering the treatment plan to the acquired CBCT and then dose re-calculation was performed in Eclipse using a CBCT-specific HU calibration curve. For the solid water measurement, the dose plane at the position of the film was exported for comparison. For each pipe measurement, the rectum pipe was contoured on the CBCT image. RT-Structure and RT-Dose DICOM files of each setup scenario were exported to enable the DSM calculations.

DSMs were calculated using the Python package *rtdsm* [29], previously developed and published under an open-source license by our group. *rtdsm* allows for two DSM calculation styles: the 'planar' approach, which samples dose using parallel axial slices, and the 'non-coplanar' approach, which uses slices angled orthogonally to the rectum's central axis path. We opted to use the non-coplanar approach as it is more appropriate for rectum structures, though we did also investigate the planar approach for comparison purposes. To begin the DSM calculation process in rtdsm, 91 slices were defined every 1.5 mm along the length of each rectum pipe contour, orthogonal to the pipe's central axis, with the central slice located at the halfway point. Next, equiangular sampling points were defined every 6.3° (for constant diameter scenarios) or 6° (for the changing diameter scenario, in order to explicitly include sampling points at the four cardinal angles) around each slice's circumference and the point dose sampled from the 3D dose matrix. Finally, the tubular dose

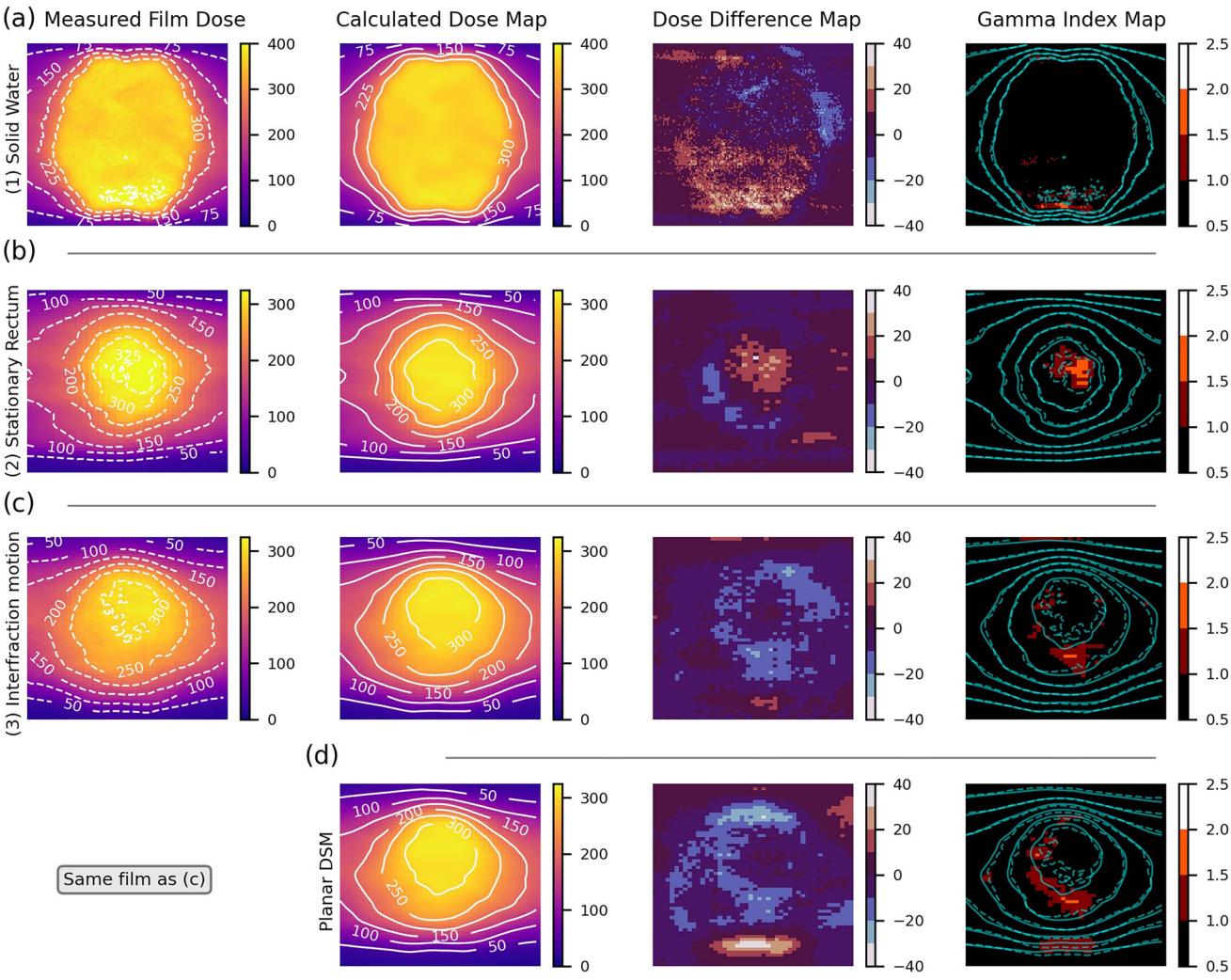

Figure 2. Total accumulated dose distributions for each measurement scenario, as measured by film and calculated DSMs, along with their gamma index maps for the 3%/2 mm criteria. Isodose lines are included to facilitate visual comparison of the film and DSM dose distributions.

distributions were cut open posteriorly and flattened into 2D dose arrays with a point resolution on the reference (smallest) pipe of 1.61 × 1.5 mm, and 1.52 × 1.5 mm for the diameter changing scenario. Accumulated doses were calculated by superimposing and adding up all single fraction DSMs for a given measurement scenario and saved as DICOM dose planes for easy import into FilmQA Pro.

In addition to the DSMs defined above, for comparison purposes, planar DSMs were also used to produce an accumulated DSM for the inter-fraction motion scenario. In this case, axial slices were simply defined every 1.5 mm along the superior-inferior axis of the CBCT image. This accumulated DSM allowed us to evaluate the accuracy of DSM accumulation using planar DSMs compared to non-coplanar ones.

Analysis

Calculated accumulated DSMs were imported into FilmQA PRO and aligned with the film measurements using the application's alignment optimization tool. Regions of comparison excluded the outer 0.5 cm of the films where water is known to irreversibly impact optical density [27]. Gamma analysis [30] was performed on the red channel with a 3% dose difference (global normalization to maximum film dose) and 2 mm distance-to-agreement using a dose threshold of 10% in accordance with TG-218 recommendations [31]. Performance was compared to TG-218's universal tolerance and action limits of ≥95% and ≥90%, respectively. Additional comparisons were also performed with 2%/2 mm and 3%/3 mm criteria to evaluate performance under stricter and more lenient conditions.

As the majority of DSM-based dose-outcome models are based on isodose region features, we also compared the similarity of isodose regions between measured and calculated surface dose. Mean distance to agreement (MDA), as well as change in isodose cluster percent area, lateral span, and longitudinal span were calculated between films and DSMs for scenarios 2 and 3 for the 150, 200, 250, and 300 cGy isodose regions. Scenario 4 was excluded from analysis due to measured dose being limited to the four profiles.

Results

Results for each experimental setup are described below, graphically presented in Figures 2 and 3, and tabulated in Table 1.

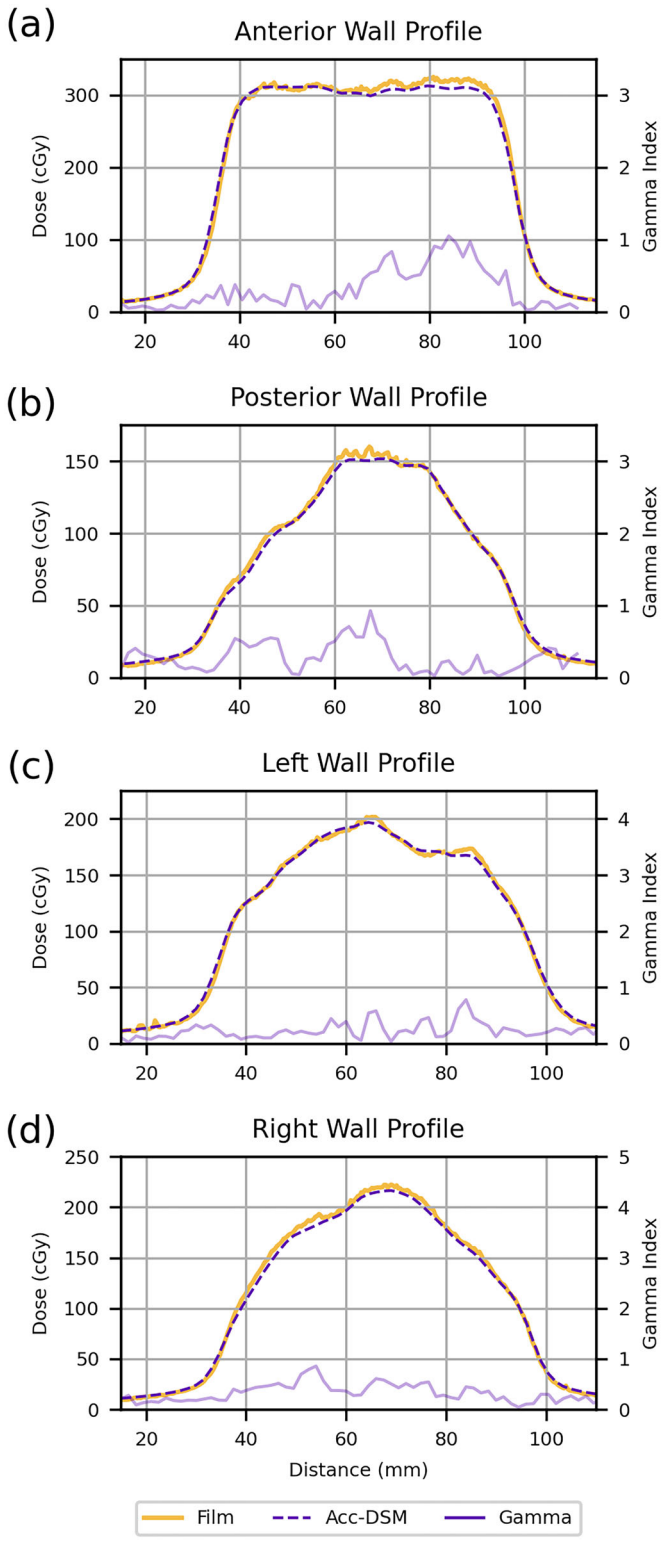

Figure 3. Dose profiles for the (a) anterior, (b) posterior, (c) left, and (d) right walls of the rectum phantom in the volume changing scenario. Gamma index values for the 3%/2 mm criteria are included. Both DSM- and DIR-based results are shown.

Dose plane in solid water

Measured and calculated delivered dose distributions at the central plane of the PTV are shown in Figure 2a along with the corresponding gamma index map. Although gamma pass rates were within action limits (98.2%, Table 1), the measured and calculated delivered dose planes disagreed in several areas. Notable hotspots exceeding 400 cGy existed within the PTV region of the film measurements that were not present in the calculated dose plane and were the main cause of gamma index failures.

Dose to a stationary rectum

Measured and DSM-calculated doses to the stationary rectum had a gamma pass rate of 95.6%, within TG-218 tolerance limits (Table 1), and with good positional agreement of all isodose lines below the prescription dose (Figure 2b). Like the previous comparison, the main source of disagreement was due to the film measuring higher dose hotspots within the PTV compared to the calculated DSM.

Dose to a rectum with inter-fraction motion

Gamma analysis of the inter-fraction motion measurements had slightly lower agreement between the film and DSM dose maps (gamma pass rate: 94.9%, Table 1), but still comfortably within TG-218 action limits. Film measurements reported lower doses than the accumulated DSM in this scenario, with the measured 300 cGy region being smaller and more contained than the calculation (Figure 2c). This influenced gamma indices in such a way that the main locations of failure occurred between the 250 and 300 cGy isodose regions, rather than within hotspots as was the case for the previous two measurements.

Film-DSM agreement decreased when using the planar style of DSM calculation (92.0% pass rate). Increased patches of disagreement were still present within the 250 cGy area as for the non-coplanar style, but also in the anterior low-dose gradient region of the inferior rectum (Figure 2d).

Dose to a rectum with inter-fraction volume changes

Dose profiles as measured with the film and extracted from the DSMs are presented in Figure 3 along with profiles of their gamma indices. Overall agreement was very strong for all four profiles (98%, Table 1), with the posterior, left, and right profiles closely matching even with stricter passing criteria. Similar to the other measurements, gamma criteria failures were primarily located in the anterior rectum, where the film measured higher doses. For example, gamma failures occurred from 80–90 mm along the anterior profile for the 2%/2 mm test.

Similarity of isodose regions

Figure 4 shows the MDA and difference between measured and calculated isodose cluster features for the examined dose thresholds. In general, sub-prescription dose clusters agreed within DSM pixel resolution (Figure 4a) and their features agreed within 4%, with the exception of scenario 2's 200 cGy lateral span (Figure 4c). On average, measured and calculated isodose clusters were least similar for the prescription dose level (300 cGy) and scenario 3's planar DSM.

Table 1. Gamma pass rates for each combination of experimental set-up and test criterion.

Experimental set-up	2%/2 mm	3%/2 mm	3%/3 mm
(1) Dose plane in solid water	98.2%	98.6%	99.2%
(2) No inter-fraction changes	90.8%	95.6%	98.1%
(3) Inter-fraction motion	87.9%	94.9%	98.8%
(3) Inter-fraction motion – Planar DSM	82.7%	92.0%	97.5%
(4) Inter-fraction volume changes – Anterior profile	86.5%	98.1%	98.1%
(4) Inter-fraction volume changes – Posterior profile	98.1%	100%	100%
(4) Inter-fraction volume changes – Left profile	98.1%	100%	100%
(4) Inter-fraction volume changes – Right profile	98.0%	100%	100%

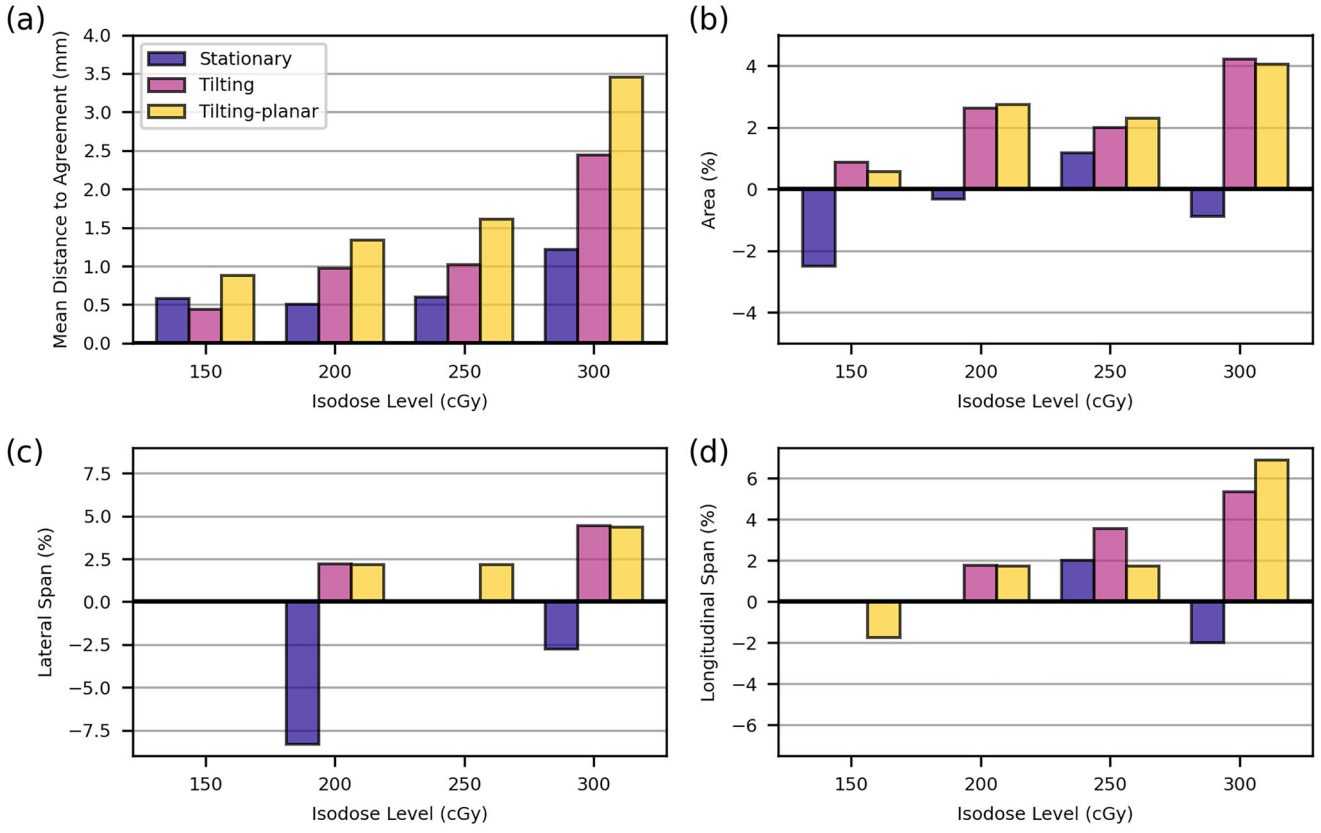

Figure 4. Comparison of isodose cluster size and shape features between film measurements and accumulated DSMs. (a) MDA; (b) difference in cluster area, (c) difference in cluster lateral span, (d) difference in cluster longitudinal span.

Discussion

The need for accurate dose accumulation methods has been recognized as a critical factor to improve understanding of normal tissue response to radiation [32]. In parallel, the value of including spatial-dose information in dose-outcome research has been demonstrated through the discovery of radiosensitive subregions that are otherwise masked by DVH metrics [7,33,34]. While a handful of studies have attempted to combine dose accumulation and spatial-dose visualization through DSM accumulation [3–7], the real-world validity of this approach has not been evaluated until now.

In this work, we tested the accuracy of DSM-based dose accumulation for rectum structures against film measurements and found good agreement between measured and calculated surface doses. Gamma pass rates using the 3%/2 mm criteria ranged from 92.0–95.6% for full surfaces and exceeded 98% for 1D profiles, falling comfortably within TG-218 recommended action limits and ranges reported by recent end-to-end performance studies of MRI guided adaptive radiotherapy (MRgART) using DIR. For example, Hoffmans and Bohoudi used film to compare measured and MRgART calculated dose to the rectum's surface for multi-fraction treatments to deformable pelvis phantoms and reported pass rates between 87.9–100% for 3%/2 mm criteria [35,36]. A similar study by Elter et al. employing gel dosimetry reported lower pass rates of 93.7% (3%/3 mm) for rectum dose, likely due to a full 3D volumetric comparison [37]. We found that agreement between film and accumulated DSMs was weakest for hotspots within the PTV (scenarios 2 and 4) and for locations in the high-dose gradient region with large inter-fraction motion (scenario 3). These may have been a consequence of positional uncertainties in regions with steeper dose gradients, similar to results observed by Marot et al. using an anthropomorphic phantom [38].

We also observed diminished agreement between film and accumulated DSMs for near-prescription isodose clusters, with MDA and feature differences beginning to exceed pixel resolution and 5%, respectively. This is noteworthy, as many DSM-based outcome-prediction models are derived using

isodose cluster features [1,4,39]. However, it is unclear what, if any, influence this may have on model performance as moderate-dose cluster features are generally the most predictive of rectal toxicities and used as model parameters more frequently than high-dose features [1,40,41]. Furthermore, accumulated isodose cluster features are likely more similar than planned features to those of the true delivered dose distribution based on previous model comparisons [4,6,7], suggesting accumulated DSMs may improve model accuracy even with some underlying inaccuracies.

Our results show that agreement between film and DSM reduces when using the simplified 'planar' style of DSM calculation for the inter-fraction motion scenario. Due to the simplified axial orientation of the DSM slices, doses to the anterior and posterior rectal walls are sampled at different locations, producing a DSM grid that displaces measured point doses relative to their film counterparts. While this displacement was kept within 1.6 mm for the scenarios of this study, displacements exceeding 3 mm are possible for angular offsets as small as 13 degrees. This poses a major potential issue for planar-style DSM accumulation accuracy for rectums with significant trajectory in the anterior-posterior or left-right directions and may have consequences for existing DSM accumulation studies. To date, all but one [6] of the DSM accumulation studies reported in the literature has used the planar calculation approach [3–5,7,22], meaning all are likely to include this effect. While we found one dissertation [22] that did provide anecdotal accounts of good correspondence between DSMs from DIR and DSM accumulation, full details of this investigation were not provided.

Although our study provides evidence for the validity of DSM-based dose accumulation for simple inter-fraction motion and deformations, further studies utilizing deformable phantoms are warranted to investigate more advanced scenarios. Particular scenarios of interest include the introduction of organ curvature changes and longitudinally-localized diameter expansions over the course of treatment. While we expect the non-coplanar DSM calculation process to correctly adjust the DSM sampling mesh better than the planar approach, experimentation is required to quantify achievable accuracy. Additionally, experiments to quantify the anisotropy of circumferential rectal wall expansion must be performed, as current DSM calculation standards assume isotropy. Should significant anisotropy exist, DSM accumulation performance is expected to reduce, and its applicability be limited in expansion scenarios. Such investigations could be conducted with phantoms or biomechanical rectum models.

In summary, the accuracy of DSM-based dose accumulation has been experimentally quantified for the first time. DSM accumulation for rectum structures showed good agreement with film measurements for simple inter-fraction motion scenarios. Provided the non-coplanar calculation method is used, DSM-based dose accumulation may be a viable alternative to DIR-based dose accumulation.

Acknowledgments

The authors gratefully acknowledge Joe Larkin for his assistance constructing the experimental phantom, Saad Aldelaijan for helpful discussions on film dosimetry, and Russel Ruo for his expertise with FilmQA Pro. HMP acknowledges funding from the Fonds de recherche du Quebec - Sante in the form of a Doctoral Training Award, as well as partial support by the CREATE Responsible Health and Healthcare Data Science (SDRDS) grant of the Natural Sciences and Engineering Research Council. JK acknowledges support from the Canada Foundation for Innovation John R. Evans Leaders Fund. We also acknowledge the logistical support provided by our colleagues in the Department of Medical Physics and the Division of Radiation Oncology at the McGill University Health Centre.

Disclosure statement

No potential conflict of interest was reported by the author(s).

Funding

This study was supported by the Fonds de Recherche du Québec - Santé; Natural Sciences and Engineering Research Council of Canada.

ORCID

H. M. Patrick http://orcid.org/0000-0002-2832-9962
J. Kildea http://orcid.org/0000-0002-7084-1425

Data availability statement

The data that support the findings of this study are available from the corresponding author, HMP, upon reasonable request.

References

[1] Buettner F, Gulliford SL, Webb S, et al. Using dose-surface maps to predict radiation-induced rectal bleeding: a neural network approach. Phys Med Biol. 2009;54(17):5139–5153. doi: 10.1088/0031-9155/54/17/005.

[2] Wortel RC, Witte MG, van der Heide UA, et al. Dose–surface maps identifying local dose–effects for acute gastrointestinal toxicity after radiotherapy for prostate cancer. Radiother Oncol. 2015;117(3):515–520. doi: 10.1016/j.radonc.2015.10.020.

[3] Scaife JE, Thomas SJ, Harrison K, et al. Accumulated dose to the rectum, measured using dose-volume histograms and dose-surface maps, is different from planned dose in all patients treated with radiotherapy for prostate cancer. Br J Radiol. 2015;88(1054):20150243. doi: 10.1259/bjr.20150243.

[4] Shelley LE, Scaife JE, Romanchikova M, et al. Delivered dose can be a better predictor of rectal toxicity than planned dose in prostate radiotherapy. Radiother Oncol. 2017;123(3):466–471. doi: 10.1016/j.radonc.2017.04.008.

[5] Murray J, McQuaid D, Dunlop A, et al. SU-E-J-14: a novel approach to evaluate the dosimetric effect of rectal variation during image guided prostate radiotherapy. Med Phys. 2014;41(6Part6):157–157. doi: 10.1118/1.4888065.

[6] Shelley LE, Sutcliffe MP, Thomas SJ, et al. Associations between voxel-level accumulated dose and rectal toxicity in prostate radiotherapy. Phys Imaging Radiat Oncol. 2020;14:87–94. doi: 10.1016/j.phro.2020.05.006.

[7] Casares-Magaz O, Bülow S, Pettersson NJ, et al. High accumulated doses to the inferior rectum are associated with late gastrointestinal toxicity in a case-control study of prostate cancer patients treated with radiotherapy. 2019;58(10):1543–1546.

[8] van Herk M, Bruce A, Guus Kroes AP, et al. Quantification of organ motion during conformal radiotherapy of the prostate by three dimensional image registration. Int J Radiat Oncol Biol Phys. 1995;33(5):1311–1320. doi: 10.1016/0360-3016(95)00116-6.

[9] Crook JM, Raymond Y, Salhani D, et al. Prostate motion during standard radiotherapy as assessed by fiducial markers. Radiother Oncol. 1995;37(1):35–42. doi: 10.1016/0167-8140(95)01613-L.
[10] Balter J, Sandler HM, Lam K, et al. Measurement of prostate motion over the course of radiotherapy. Int J Radiat Oncol Biol Phys. 1993;27:223. doi: 10.1016/0360-3016(93)90784-S.
[11] Zelefsky MJ, Kollmeier M, Cox B, et al. Improved clinical outcomes with high-dose image guided radiotherapy compared with non-IGRT for the treatment of clinically localized prostate cancer. Int J Radiat Oncol Biol Phys. 2012;84(1):125–129
[12] Marcello M, Ebert M, Haworth A, et al. Association between treatment planning and delivery factors and disease progression in prostate cancer radiotherapy: results from the TROG 03.04 RADAR trial. Radiother Oncol. 2018;126(2):249–256. doi: 10.1016/j.radonc.2017.10.021.
[13] Heemsbergen WD, Al-Mamgani A, Witte MG, et al. Radiotherapy with rectangular fields is associated with fewer clinical failures than conformal fields in the high-risk prostate cancer subgroup: results from a randomized trial. Radiother Oncol. 2013;107(2):134–139. doi: 10.1016/j.radonc.2013.03.019.
[14] Wortel RC, Incrocci L, Pos FJ, et al. Acute toxicity after Image-Guided intensity modulated radiation therapy compared to 3D conformal radiation therapy in prostate cancer patients. Int J Radiat Oncol Biol Phys. 2015;91(4):737–744. doi: 10.1016/j.ijrobp.2014.12.017.
[15] van Haaren PM, Bel A, Hofman P, et al. Influence of daily setup measurements and corrections on the estimated delivered dose during IMRT treatment of prostate cancer patients. Radiother Oncol. 2009;90(3):291–298. doi: 10.1016/j.radonc.2008.12.021.
[16] Thornqvist S, Petersen JB, Hoyer M, et al. Propagation of target and organ at risk contours in radiotherapy of prostate cancer using deformable image registration. Acta Oncol. 2010;49(7):1023–1032. doi: 10.3109/0284186X.2010.503662.
[17] Thor M, Petersen JB, Bentzen L, et al. Deformable image registration for contour propagation from CT to cone-beam CT scans in radiotherapy of prostate cancer. Acta Oncol. 2011;50(6):918–925. doi: 10.3109/0284186X.2011.577806.
[18] Gao S, Zhang L, Wang H, et al. A deformable image registration method to handle distended rectums in prostate cancer radiotherapy. Med Phys. 2006;33(9):3304–3312. doi: 10.1118/1.2222077.
[19] Velec M, Moseley JL, Svensson S, et al. Validation of biomechanical deformable image registration in the abdomen, thorax, and pelvis in a commercial radiotherapy treatment planning system. Med Phys. 2017;44(7):3407–3417. doi: 10.1002/mp.12307.
[20] Kadoya N, Miyasaka YY, Yamamoto T, et al. Evaluation of rectum and bladder dose accumulation from external beam radiotherapy and brachytherapy for cervical cancer using two different deformable image registration techniques. J Radiat Res. 2017;58(5):720–728. doi: 10.1093/jrr/rrx028.
[21] Motegi K, Tachibana H, Motegi A, et al. Usefulness of hybrid deformable image registration algorithms in prostate radiation therapy. J Appl Clin Med Phys. 2019;20(1):229–236. doi: 10.1002/acm2.12515.
[22] D'Aquino A. Assessment of delivered rectal dose in prostate cancer radiotherapy [dissertation]. University of London; 2021. Available from: https://repository.icr.ac.uk/handle/internal/4878
[23] Yeo UJ, Taylor ML, Supple JR, et al. Is it sensible to "deform" dose 3D experimental validation of dose-warping. Med Phys. 2012;39(8):5065–5072. doi: 10.1118/1.4736534.
[24] De Crevoisier R, Tucker SL, Dong L, et al. Increased risk of biochemical and local failure in patients with distended rectum on the planning CT for prostate cancer radiotherapy. Int J Radiat Oncol Biol Phys. 2005;62(4):965–973.
[25] Barbosa Neto O, Souhami L, Faria S. Hypofractionated radiation therapy for prostate cancer: the McGill university health center experience. Cancer Radiother. 2015;19(6–7):431–436. doi: 10.1016/j.canrad.2015.05.015.
[26] Agazaryan N, Solberg TD, DeMarco JJ. Patient specific quality assurance for the delivery of intensity modulated radiotherapy. J Appl Clin Med Phys. 2003;4(1):40–50. doi: 10.1120/jacmp.v4i1.2540.
[27] Aldelaijan S, Devic S, Mohammed H, et al. Evaluation of EBT-2 model GAFCHROMIC^{TM} film performance in water. Med Phys. 2010;37(7):3687–3693. doi: 10.1118/1.3455713.
[28] Lewis D, Micke A, Yu X, et al. An efficient protocol for radiochromic film dosimetry combining calibration and measurement in a single scan. Med Phys. 2012;39(10):6339–6350. doi: 10.1118/1.4754797.
[29] Patrick HM, Kildea J. Technical note: rtdsm-An open-source software for radiotherapy dose-surface map generation and analysis. Med Phys. 2022;49(11):7327–7335. doi: 10.1002/mp.15900.
[30] Low DA, Harms WB, Mutic S, et al. A technique for the quantitative evaluation of dose distributions. Med Phys. 1998;25(5):656–661. doi: 10.1118/1.598248.
[31] Miften M, Olch A, Mihailidis D, et al. Tolerance limits and methodologies for IMRT measurement-based verification QA: recommendations of AAPM task group no. 218. Med Phys. 2018;45(4):e53–e83. doi: 10.1002/mp.12810.
[32] Jaffray DA, Lindsay PE, Brock KK, et al. Accurate accumulation of dose for improved understanding of radiation effects in normal tissue. Int J Radiat Oncol Biol Phys. 2010;76(3 SUPPL):S135–S9. doi: 10.1016/j.ijrobp.2009.06.093.
[33] Acosta O, Drean G, Ospina JD, et al. Voxel-based population analysis for correlating local dose and rectal toxicity in prostate cancer radiotherapy. Phys Med Biol. 2013;58(8):2581–2595. doi: 10.1088/0031-9155/58/8/2581.
[34] Palorini F, Cozzarini C, Gianolini S, et al. First application of a pixel-wise analysis on bladder dose-surface maps in prostate cancer radiotherapy. Radiother Oncol. 2016;119(1):123–128. doi: 10.1016/j.radonc.2016.02.025.
[35] Hoffmans D, Niebuhr N, Bohoudi O, et al. An end-to-end test for MR-guided online adaptive radiotherapy. Phys Med Biol. 2020;65(12):125012. doi: 10.1088/1361-6560/ab8955.
[36] Bohoudi O, Lagerwaard FJ, Bruynzeel AM, et al. End-to-end empirical validation of dose accumulation in MRI-guided adaptive radiotherapy for prostate cancer using an anthropomorphic deformable pelvis phantom. Radiother Oncol. 2019;141:200–207. doi: 10.1016/j.radonc.2019.09.014.
[37] Elter A, Dorsch S, Mann P, et al. End-to-end test of an online adaptive treatment procedure in MR-guided radiotherapy using a phantom with anthropomorphic structures. Phys Med Biol. 2019;64(22):225003. doi: 10.1088/1361-6560/ab4d8e.
[38] Marot M, Elter A, Mann P, et al. Technical note: on the feasibility of performing dosimetry in target and organ at risk using polymer dosimetry gel and thermoluminescence detectors in an anthropomorphic, deformable, and multimodal pelvis phantom. Med Phys. 2021;48(9):5501–5510. doi: 10.1002/mp.15096.
[39] Vanneste BG, Buettner F, Pinkawa M, et al. Ano-rectal wall dose-surface maps localize the dosimetric benefit of hydrogel rectum spacers in prostate cancer radiotherapy. Clin Transl Radiat Oncol. 2019;14:17–24. doi: 10.1016/j.ctro.2018.10.006.
[40] Moulton CR, House MJ, Lye V, et al. Spatial features of dose-surface maps from deformably registered plans correlate with late gastrointestinal complications. Phys Med Biol. 2017;62(10):4118–4139. doi: 10.1088/1361-6560/aa663d.
[41] Casares-Magaz O, Muren LP, Moiseenko V, et al. Spatial rectal dose/volume metrics predict patient-reported gastro-intestinal symptoms after radiotherapy for prostate cancer. Acta Oncol. 2017;56(11):1507–1513. doi: 10.1080/0284186X.2017.1370130.